Beclin-mediated autophagy drives dorsal longitudinal flight muscle histolysis in the variable field cricket, *Gryllus lineaticeps*

Tomás Diaz[1], Lisa A. Treidel[2], Michael A. Menze[3], Caroline M. Williams[1], Jacqueline E. Lebenzon[1]*

[1]Department of Integrative Biology, University of California Berkeley, 2040 Valley Life Sciences Building, Berkeley, CA 94720, USA

[2]School of Biological Sciences, University of Nebraska Lincoln, 1104 T Street, Lincoln, NE 68588, USA

[3]Department of Biology, University of Louisville, 139 Life Sciences Bldg. Louisville, KY 40292, USA

***Author for correspondence**: Jacqueline Lebenzon, jlebenzon@berkeley.edu

Other authors' emails: tomasdiaz@berkeley.edu (TD), ltreidel2@unl.edu (LAT), michael.menze@louisville.edu (MAM), cmw@berkeley.edu (CMW)

Keywords: Muscle breakdown, insect dispersal, life history trade-off, RNAi, *beclin*-mediated autophagy, Gryllus, histolysis

Running title: Autophagy drives flight muscle histolysis in crickets

ABSTRACT

Flight muscle histolysis is a widespread strategy used by insects to break down functional flight muscle and modulate the energetic costs associated with flight muscle use and maintenance. The variable field cricket, *Gryllus lineaticeps*, undergoes histolysis during their transition between dispersal flight and reproduction. Despite the importance of histolysis on insect reproduction and fitness, the molecular mechanisms driving this flight muscle breakdown are not well understood. Here, we show that *beclin*-mediated autophagy, a conserved lysosomal-dependent degradation process, drives breakdown of dorsal longitudinal flight muscle in female flight capable *G. lineaticeps*. We found that female *G. lineaticeps* activate autophagy in their dorsal longitudinal flight muscle (DLM) during histolysis, but not in the neighboring dorsoventral flight muscle (DVM), which remains functional. RNA interference knockdown of *beclin*, a gene which encodes a critical autophagy initiation protein, delayed DLM histolysis, but did not affect DVM histolysis. This suggests that crickets selectively activate autophagy to break down the DLMs, while maintaining DVM function for other fitness-relevant activities such as walking. Overall, we confirmed that autophagy is a critical pathway used to remodel flight muscle cells during flight muscle histolysis, illuminating for the first time the mechanisms underlying a major life history transition between dispersal and reproduction.

INTRODUCTION

Tissue remodeling is commonly observed in metazoans (Pinet and McLaughlin 2019), and many animals have evolved the capacity to match muscle function and structure with varying energetic demands of their life cycle. Skeletal muscles are key to locomotor performance and dispersal, making the ability to grow and maintain muscle crucial for increasing organismal fitness (Irschick and Garland 2001). For example, migratory birds undergo massive hypertrophy of their flight muscles to power long-haul flights between wintering and breeding grounds (Price et al. 2011; Young et al. 2021); and hibernating ground squirrels resist skeletal muscle atrophy to preserve locomotor ability throughout the winter, despite significant reductions in skeletal muscle contraction and lack of food for months at a time (Zhang et al. 2016; Goropashnaya et al. 2020). However, growing, maintaining and using skeletal muscle is energetically expensive and involves producing and expending vast amounts of ATP to maintain and restore muscle cell membrane potentials, power myosin ATPase activity, facilitate active calcium reuptake, and synthesize muscle protein (Romanello and Sandri 2016). Insect flight muscle is particularly costly to use and maintain, and the energetic costs of flight muscles cause resource-based trade-offs that limit early-life fecundity (Zera et al. 1997; Nespolo et al. 2008; Iwamoto 2011). Many insects have evolved the ability to degrade their flight muscle altogether prior to the onset of reproduction, in a process known as muscle histolysis (Marden 2000).

Flight muscle histolysis is an evolutionarily important process present in at least five orders of insects (Coleoptera, e.g. Lebenzon et al. 2022; Hemiptera, e.g. Kaitala and Hulden 1990; Hymenoptera, e.g. Matte and Billen 2021; Orthoptera, e.g. Zera et al. 1997; Lepidoptera, e.g. Cheng et al. 2016), which enables organisms to adaptively reallocate energy away from dispersal within their life cycle. For example, diapausing Colorado potato beetles degrade their flight muscle during winter, which drives lower metabolic rates and higher energy savings during

periods of low resource availability when they do not need to fly (Lebenzon et al. 2022). In many seasonally migrating and wing dimorphic insects, flight muscle histolysis coordinates the cessation of dispersal and reallocation of energy towards reproductive development (Zera et al. 1997; Roff and Fairbairn 2007; Stahlschmidt 2022). In the latter example, timing of histolysis appears to modulate trade-offs of the "flight-oogenesis syndrome" in females, such that breakdown products from the flight muscle (i.e. amino acids) could be used as substrates directly for oogenesis (Wheeler 1996; Lorenz 2007; Treidel et al. 2021). Despite the importance of flight muscle histolysis on insect reproduction and fitness, we understand relatively little about the underlying mechanisms driving this muscle breakdown. Further, the ability to selectively degrade a single muscle type is a unique insect trait; most other vertebrate taxa maintain or grow their muscles where possible, and any observed muscle breakdown and atrophy is simply a pathological consequence of aging or disuse (Wall et al. 2013; Larsson et al. 2019). Thus, understanding the mechanisms underlying muscle histolysis could contribute to a broader understanding of how muscle plasticity has evolved to combat energetic challenges.

Flight muscle histolysis is often associated with protein degradation. For example, the house cricket, *Acheta domesticus*, reduces the expression of genes that encode crucial muscle protein [notably troponin and actin; Lu et al. 2023) during histolysis, and there is a pattern of overall lower protein content in histolyzed muscle of several species of Gryllus field crickets (Zera et al. 1997; Lorenz 2007). Flight muscle histolysis in diapausing Colorado potato beetles not only involves the degradation of muscle protein but also widespread degradation of flight muscle mitochondria through mitophagy, mitochondrion-specific autophagy (Lebenzon et al. 2022). Given these observed patterns of protein degradation in crickets and beetles, autophagy

could play a ubiquitous role in driving insect muscle histolysis, especially in species where histolysis coordinates life history transitions associated with reduced investment into dispersal.

Autophagy is a conserved lysosomal-dependent pathway that degrades and recycles intracellular proteins and organelles (Mizushima 2007). Proteins and organelles destined for degradation are tagged by ubiquitin ligases, and then recognized and surrounded by a suite of autophagy-related proteins (ATG proteins) including GABARAPL (ATG8 family) and Beclin (ATG6 family). ATG proteins are required to initiate and aid in the formation of a double-membraned autophagosome that engulfs and sequesters cargo destined for degradation (Sun et al. 2009; Schaaf et al. 2016). Autophagosomes then fuse with lysosomes to form an autolysosome, where the cargo will eventually be degraded, and the macromolecules will be recycled (Mizushima 2007). Autophagy is especially important for nutrient recycling in energy-stressed cells and is partially regulated by upstream energy-sensing pathways (e.g. mTOR and AMPK signaling; Kim et al. 2011). Thus, we hypothesize that autophagy facilitates the breakdown of proteins for energy reallocation during insect flight muscle histolysis.

Here, we explored the putative role of autophagy in driving flight muscle histolysis of adult female, flight-cabable variable field crickets, *Gryllus lineaticeps* (Stål 1858). *Gryllus lineaticeps* are a common field cricket found throughout the Western United States and are an emerging model system for studying the physiological basis of flight-fecundity trade-offs. Flight-capable *G. lineaticeps* emerge at the start of adulthood with fully developed long wings and large functional flight muscles (Treidel et al. 2021, 2023). Flight-capable females invest in flight muscle maintenance and prepare for flight by accumulating large somatic lipid stores, but delay reproduction and ovarian development until the end of the first week of adulthood. Muscle histolysis of the flight muscles is closely tied to the onset of oogenesis in female flight-capable

crickets, such that ovary mass only substantially increases once histolysis is initiated (Treidel et al. 2021). Timing of flight muscle histolysis is controlled by integrated nutritional and neuroendocrine signaling pathways, but histolysis occurs eventually in all individuals regardless of environmental conditions, suggesting that histolysis is required for females of this species to reach their full reproductive potential (Zera et al. 1998; Shiga et al. 2002; Treidel et al. 2021). Thus, *G. lineaticeps* is a powerful model to better understand the precise mechanisms underlying the cellular changes required for flight muscle histolysis in the context of reproductive onset.

Muscle histolysis in flight-capable *G. lineaticeps* results in the breakdown of both major sets of thoracic flight muscles in Orthopterans – the dorsal longitudinal muscles (DLM), which produce the power stroke of flight by depressing the wing, and the bifunctional dorsoventral muscles (DVM), which produce the upstroke of wings in flight and control leg movement during walking (Wilson 1962; Treidel et al. 2022). The downstream molecular processes driving the selective degradation of these muscles are unknown. We begin to address this gap by testing the hypothesis that autophagy is activated during histolysis of both sets of flight muscles (DLM and DVM). We tested this first by using electron microscopy to visualize potential autophagic structures in histolyzing flight muscles, and then by measuring the expression of *beclin* (a gene encoding an important autophagy initiator; Cao and Klionsky 2007) during histolysis. We then established a causal role of *beclin*-mediated autophagy in flight muscle histolysis by knocking down *beclin* transcript abundance in female flight-capable crickets using RNA interference. If *beclin*-mediated autophagy is necessary for muscle histolysis, we predicted that knocking down *beclin* would 1) prevent autophagy activation and thus 2) prevent or delay muscle histolysis. Further, if autophagy is necessary for both histolysis and the resulting onset of oogenesis, then knocking down *beclin* should also delay oogenesis in adult female flight capable crickets. Our

study is the first to experimentally determine autophagy's role in orthopteran flight muscle histolysis, and provides new insights into how organisms can use autophagy to coordinate transitions and allocations of energy between expensive life history traits.

MATERIALS & METHODS

Cricket Rearing and maintenance

Variable field crickets, *G. lineaticeps*, were reared as described in Treidel et al. (2023). Briefly, laboratory colonies at UC Berkeley (Berkeley, CA, USA) were kept at approximately 27 °C with a light: dark cycle of 16 h: 8 h and given *ad libitum* access to water and a standard diet composed of wheat bran, wheat germ, milk powder, and nutritional yeast. Each week, new reproductively mature adults are added into breeding colonies maintained at a 50:50 ratio of wing morph (50% long wing, 50% short wing) and provided with wet substrate (mixture of soil and sand) for oviposition in plastic cups. After 1 week, the egg cups were removed and placed in individual plastic containers to develop and hatch. For all experiments, we isolated adult flight capable (long winged) female crickets from cages of juvenile crickets on their day of emergence, which we deem "Day 0". These individuals were subsequently housed in individual plastic containers, in the same environmental conditions, with *ad libitum* access to water and food.

Experimental framework and flight muscle color classification

The timing of muscle histolysis in *G. lineaticeps* was previously established by Treidel et al. (2021). When females emerge (Day 0), both types of flight muscle (DLM and DVM) are large in mass and appear red in color. Most female crickets histolyze their flight muscle by day 5 of adulthood, which is concurrent with a reduction in muscle mass and a red-to-white color

transition (Treidel et al. 2021, 2023). Here, we use muscle color as an indicator of histolysis progression and classify functional muscle as red, histolyzing muscle as pink, and histolyzed muscle as white (Figure 1). Since insects rely on simple diffusion of oxygen from tracheoles to muscles and do not have muscle myoglobin (Weis-Fogh 1964), we expect that these color changes are due to changes in cytochrome compounds as muscles histolyze. We analyzed and classified the status of DLM and DVM separately because of the putative differences in their function (DLM for flight, DVM for flight and walking) and observed differences in histolysis timing (DLM is histolyzed first; Fig. 1).

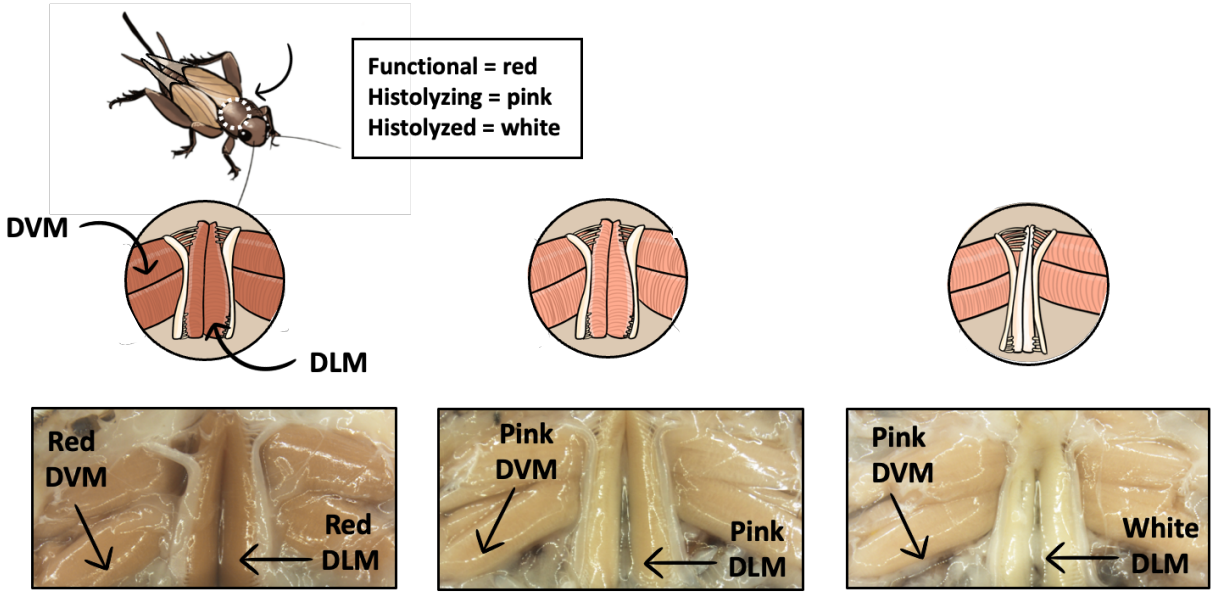

Figure 1. Flight muscle status classification in female *G. lineaticeps,* illustrating selective histolysis of the DLM muscle. Illustrations in circles show the position of the dorsal longitudinal (DLM) and dorsoventral (DVM) muscle in the cricket thorax. Photographs of each stage of muscle histolysis are shown in boxes below the illustrations, and arrows point to the color and muscle type.

Sample preparation and imaging for transmission electron microscopy

We used transmission electron microscopy to visualize any potential autophagic structures in flight muscle cells. We euthanized female long-winged crickets by decapitation, and a longitudinal incision was made on the ventral thorax and abdomen to expose the flight muscles. We then dissected histolyzing (pink) DLM and DVM from 3-day-old crickets and placed the tissues straight into ice-cold fixative (2% glutaraldehyde, 2.5% paraformaldehyde in 0.2 M sodium phosphate buffer, pH=7.4), for storage at 4 °C until staining. We only dissected from pink because if autophagy is active during histolysis, we would expect to observe autophagic structures during this "histolyzing" time point. On the day of staining, we washed the tissues (1 x 5 min, 5 x 15 mins) in double distilled water to ensure the removal of any residual fixative, and stained tissues with 1% osmium tetroxide with 1.6% potassium ferricyanide (KFeCn) at room temperature for 45 mins in the dark. Next, we washed fixed muscle samples with double distilled water (1 x 5 min, 5 x 15 min) to ensure the removal of residual osmium tetroxide and KFeCn, and then stained with 2% uranyl acetate overnight at 4 °C in the dark. We rewashed tissues (1 x 5 min, 5 x 15 min) with double distilled water to ensure the removal of excess uranyl acetate, and then serially dehydrated the tissue in acetone, and embedded them in Epon-Araldite resin that was polymerized in resin molds at 60 °C for four days. We cut 0.5 μm sections of the sample, stained each section with 2% uranyl acetate immediately followed by Reynold's lead citrate, and then finally imaged sections using an FEI Tecnai 12 Transmission Electron Microscope equipped with a Gatan Rio 16 4K CMOS camera (Gatan, Pleasanton California, USA).

193 *Quantification of* beclin *mRNA abundance during muscle histolysis*

194 We used quantitative real time PCR (qPCR) to measure changes in transcript abundance
195 of *beclin* in crickets in functional, histolyzing, and histolyzed flight muscle (Figure 1). We
196 dissected dorsal longitudinal and dorsoventral flight muscles (as described above) from five-day
197 old adult female long-winged crickets with functional (red), histolyzing (pink), and histolyzed
198 (white) muscles. Tissues were immediately flash-frozen in liquid nitrogen and stored at -80°C
199 until RNA extractions. We extracted RNA using TRIzol according to the manufacturer's
200 instructions (ThermoFisher Scientific, Emeryville, CA, USA), removed residual genomic DNA
201 using DNase (Quanta Biosciences, Beverly, MA, USA), and measured the absorbance of the
202 final preparation at $\lambda = 260$ nm and $\lambda = 280$ nm using a Nanodrop spectrophotometer
203 (ThermoFisher scientific, Mississauga, ON, Canada) to determine RNA purity and concentration.
204 We used the qScript cDNA synthesis kit (Quanta Biosciences, Beverly, MA, USA) to synthesize
205 cDNA from 1000 ng of RNA and then stored samples at -20 °C until qPCR was performed.
206 cDNA was diluted to a consistent concentration in all reactions prior to use in qPCR reactions
207 and was amplified using Applied Biosystems PowerUp SYBR Mastermix (ThermoFisher
208 Scientific, Waltham Massachusetts, USA). In each qPCR reaction, we added the forward and
209 reverse primers at a concentration of 0.4 μM and 1 μg of cDNA, and we ran each reaction in
210 triplicate on a QuantStudio 3 thermal cycler (ThermoFisher scientific, Waltham Massachusetts,
211 USA). We designed *beclin* primers (Table S1) with Primer3 software (v4.1.0,
212 https://primer3.ut.ee/) using the *beclin* mRNA sequence from the publicly available *Gryllus*
213 *bimaculatus* genome database (https://gbimaculatusgenome.rc.fas.harvard.edu/, GBI_06202-RA;
214 Ylla et al. 2021) and validated their efficiencies (to ensure 95-100% primer efficiency) as
215 described in Lebenzon et al. 2022. Transcript abundance was normalized to the expression of

two reference genes, *vesicle transport protein* (*VTP*) and calcium binding protein (*CaBP*) (validated for stability in Vellichirammal et al. 2014). Relative normalized transcript abundance was calculated using the comparative C_T ($2^{-\Delta\ \Delta CT}$) method (Livak and Schmittgen 2001), and we compared differences in mean raw C_T values among muscle states using separate one-way ANOVAs in R for DLM and DVM (version 4.3.2, R core team, Vienna Austria).

dsRNA production and validation of RNA interference knockdown of beclin

We designed and synthesized dsRNA constructs complementary to 1) *beclin*, which when introduced into crickets would elicit an RNAi response and knock down *beclin* expression and 2) green fluorescent protein (GFP) which is not complementary to any endogenous mRNA transcript in crickets and therefore acts as a negative control. We used E-RNAi software (https://www.dkfz.de/signaling/e-rnai3/; Horn and Boutros 2010) to design primers which amplified *beclin* from cricket cDNA or *GFP* from a CRISPR Universal Negative Control plasmid (Sigma Aldrich). Each primer contained a T7 promoter sequence on the 5' end, which is required for downstream dsRNA synthesis by a T7 RNA polymerase. According to the manufacturer's instructions, we used these primers to then generate templates for dsRNA from cricket cDNA and the CRISPR Universal Negative Control plasmid *via* PCR. To synthesize dsRNA, we used the MEGAScript RNAi kit (ThermoFisher Scientific, Waltham Massachusetts, USA) following the manufacturer's protocol. We incubated dsRNA reactions at 37°C for 4 hours for synthesis, performed a final nuclease digestion to remove residual DNA, and confirmed successful dsRNA synthesis by performing gel electrophoresis and observing bands at 485 bp (for *dsBeclin*) and 411 bp (for *dsGFP*) (Figures S1).

Two days after adult emergence, we injected crickets with a 10 µl Hamilton syringe (Hamilton Company, Reno, Nevada, USA) with a 30 G needle, with 1000 ng (in c. 5 µl of 1X sterile phosphate buffered saline) of either *dsBeclin* or *dsGFP*, to reduce *beclin* transcript abundance or serve as a negative control, respectively. Timing of injection (2-days post-emergence) was chosen to allow for full flight muscle development (Treidel et al. 2021). We dissected both DLM and DVM from crickets as described above two- and four-days post-dsRNA injection, to verify the extent and timing of transcript knockdown. We then used qPCR to verify transcript knockdown in both DLM and DVM samples as described above, and compared C_T values using a Student's t-test in Microsoft Excel. Data for *beclin* expression in DLM and DVM in crickets two days post-dsRNA injection are in Figure S3.

Effects of beclin *knockdown on muscle histolysis progression and autophagy-related protein abundance*

After validating our RNAi knockdown of *beclin,* we used a new subset of dsRNA-injected crickets to investigate the effects of this *beclin* knockdown on muscle histolysis progression. Adult crickets two days after emergence were weighed and then injected with *dsBeclin* or *dsGFP* as a negative control as described above. Three days after the injection, crickets were re-weighed, their ovaries were dissected and weighed, and then both muscle types were dissected as described above (Figure S2). Dorsal longitudinal and dorsoventral muscles were photographed using an SMZ18 stereomicroscope equipped with a DS-Fi3 camera (Nikon, Minato City, Tokyo, Japan) and then immediately flash-frozen in liquid nitrogen and stored at -80 °C until they were used in western blots (described below). We used muscle photographs to score muscle color as a proxy for muscle histolysis progression (Figure 1). Two authors (TD and

JEL) scored each photograph for consensus while blind to dsRNA injection treatment (*dsBeclin* or *dsGFP*). We then used a Fisher's exact test in R (v4.3.2, R core team, Vienna, Austria) to compare differences in the proportion of crickets with functional and histolyzed muscle and a Welch's t-test in Graphpad prism to compare differences in ovary mass between *dsBeclin* and *dsGFP*-injected crickets. We normalized ovary mass according to the equation $\frac{ovary\ mass\ (mg)}{body\ mass\ (mg) - ovary\ mass\ (mg)}$.

Finally, to explore fine-scale changes in flight muscle histolysis progression induced by *beclin* knockdown, we used immunoblots to assess the abundance of Cytochrome c oxidase (COX, to assess impacts of *beclin* knockdown on mitochondrial abundance; Treidel et al. 2023) and GABARALP1/2 (to assess autophagy activation; Willot et al. 2023) in the DLM of crickets (Figure S2). To extract protein, we added 300 µl of lysis buffer (1% Triton X100, 1% SDS, 1X TBS, 1mM EDTA, 1% Protease inhibitor cocktail) per 5 mg of DLM. We homogenized the samples manually using a plastic pestle, and then sonicated each sample using a handheld sonicator (1 x 10 sec; Model 50, Fisher Scientific, Hampton, New Hampshire, USA). Following sonication, samples were centrifuged (15,000 G, 10 min, 4°C) and the resulting supernatant was collected. We quantified protein using the Pierce BCA Assay Kit (ThermoFisher Scientific, Waltham, Massachusetts, USA) and then prepared samples for loading by combining 20 µg of protein in water, 5 µl LDS sample buffer (ThermoFisher Scientific, Waltham Massachusetts, USA), and 2 µl Beta-mercaptoethanol. Samples were then boiled for 10 min at 70°C and stored at -20°C until use.

We used Invitrogen Bolt Bis-Tris Plus Mini Protein Gels (4-12%, 1.0 mm, ThermoFisher Scientific, Waltham Massachusetts, USA) for electrophoretic protein separation. We loaded 20 µl of each protein sample (each containing 20 µg of protein), or 8 µl of PageRuler Prestained

NIR Protein Ladder (ThermoFisher Scientific, Waltham Massachusetts, USA) into wells of the gel and ran each gel in 1x running buffer (MES or MOPS depending on protein size of interest) at 150 V for 35 mins.

We then transferred the proteins to a polyvinylidene fluoride (PVFD) membrane at 20 V for 60 min. The membrane was washed with TBS and then incubated with Licor 700 Total protein stain (LI-COR Biosystems, Lincoln, Nebraska, USA) for 5 min. Following incubation, the membrane was imaged on an Azure c500 Imager (Azure Biosystems, Dublin, California, USA) with NIR Red (700 Channel, auto exposure). After imaging, the membrane was washed 3 times with TBS and then incubated with 6 mL of TBS Blocking Buffer (LI-COR Biosystems, Lincoln, Nebraska, USA) for 2 hours at room temperature. After incubation, the membrane was incubated in primary antibody (in 1X TBST, 0.05% BSA, 10% NaN_3) at a dilution of 1:1000 for COX-IV (Novus Biologicals NB110-39115), and 1:2000 for GABARAPL1/2 (Abcam EPR4805) overnight at 4°C. The membrane was then washed with TBST and then incubated in the secondary antibody (LI-COR Biosystems 926-32211) at a dilution of 1:10000 for one hour at room temperature. Following the incubation, the membranes were washed 2X with TBST and then 2X with TBS. Finally, the membrane was imaged with an Azure c500 Imager (Azure Biosystems, Dublin, California, USA) using NIR Red (800 Channel, auto exposure). We used ImageJ to quantify COX-IV abundance and GABARAP1/2 based on the density of bands present at c. 19 kDa (COX-IV) and c. 17 kDa/15 kDa (GABARAPL1/2). We standardized each protein sample to the total protein before statistical analysis and then used a Student's t-test in excel to compare differences in protein (COX, GABARAPL1 or GABARAPL2) abundance between *dsBeclin* and *dsGFP*-injected crickets.

RESULTS

We found that autophagic structures (lysosomes, autophagosomes and autolysosomes) are present in histolyzing dorsal longitudinal (DLM) and dorsoventral (DVM) flight muscle (Fig. 2A), suggesting that autophagy is activated in both sets of flight muscle during histolysis. *Beclin* transcript abundance increases significantly in histolyzing and histolyzed dorsal longitudinal muscle compared to functional muscle ($F_{2,15} = 52.39$, $P < 0.0001$, Fig. 2B), but does not increase significantly in dorsoventral muscle ($F_{2,15} = 2.62$, $P = 0.11$, Fig 2B).

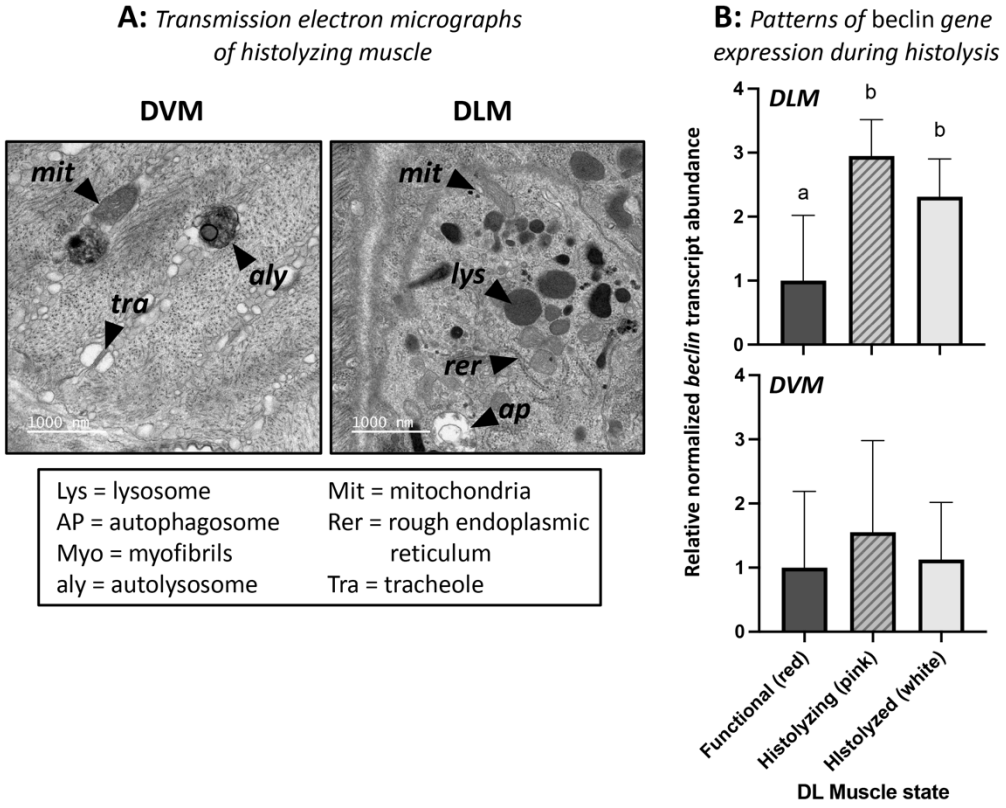

Figure 2. Crickets activate autophagy in the flight muscles during histolysis A) Transmission electron micrographs (6800x magnification) of "pink" (histolyzing) DVM (left) and DLM (right), showing the appearance of autophagy-related structures in both muscle types (autophagosomes; AP; autolysosomes, aly). B) *Beclin* expression is increased in the dorsal longitudinal muscle (DLM; top) but not dorsoventral muscle (DVM; bottom) muscles during histolysis. Data are mean ± SD normalized *beclin* abundance (n=6 crickets/muscle type/muscle state), normalized to two reference genes. Different letters denote statistically significant differences among groups according to a one-way ANOVA ($p<0.05$).

To elicit an RNAi response and knockdown the expression of *beclin*, we injected flight-capable females with *dsBeclin* (or *dsGFP* as a negative control). Four days post injection, crickets injected with *dsBeclin* had lower *beclin* transcript abundance in both their dorsoventral muscle (64% knocked down, $P = 0.019$, $t_6=-2.35$) and dorsal longitudinal muscle (72% knockdown down, $P = 0.007$, $t_6=-2.92$), compared to those injected with *dsGFP* (Fig. 3).

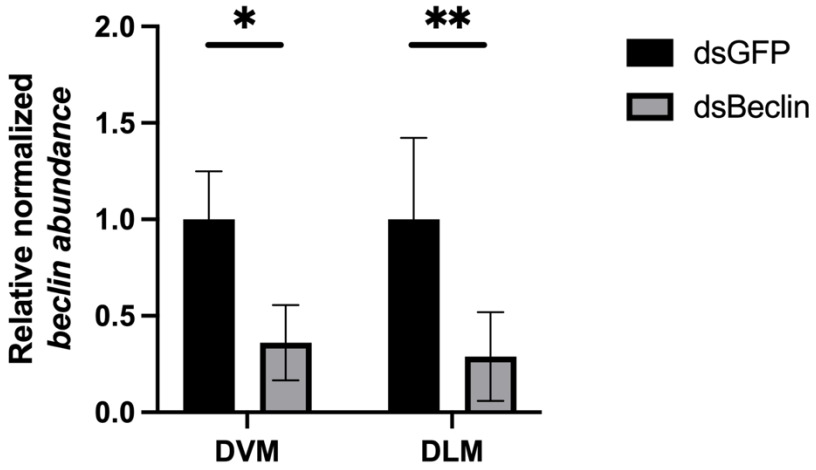

Figure 3. Verification of RNA interference knockdown of *beclin* expression in female *Gryllus lineaticeps* flight muscle *via* qPCR. Bars show mean ± SD normalized *beclin* abundance in muscles from crickets injected with either *dsGPF* (black) or *dsBeclin* (grey), four days after injection (n=6 crickets/muscle type/dsRNA injection). An asterisk is used to show a significant difference between treatments according to a Student's T-test ($P < 0.05$). DVM = Dorsoventral muscle, DLM = Dorsal longitudinal muscle.

Knocking down *beclin* transcript abundance in flight-capable female *G. lineaticeps* delayed muscle histolysis progression. A significantly higher proportion of crickets treated with *dsBeclin* maintained their dorsal longitudinal muscle (a red or pink muscle) compared to those treated with *dsGFP* (Fisher's exact test, $P = 0.033$). 21% of *dsBeclin*-injected crickets had red muscle, 29% had pink muscle, and only 50% had white muscle (Fig. 4A). In comparison, only 13% of *dsGFP*-injected crickets had red muscle, 13% had pink muscle, and 73% had white muscle (Fig 4A). Dorsoventral muscle of crickets, regardless of treatment, were maintained at similar levels (Fisher's exact test, $P = 0.57$, Fig. 4B). We found no significant differences in ovary mass in crickets injected with *dsBeclin* or *dsGFP* ($P = 0.8851$, $t_{27}=0.15$. Fig. 4C).

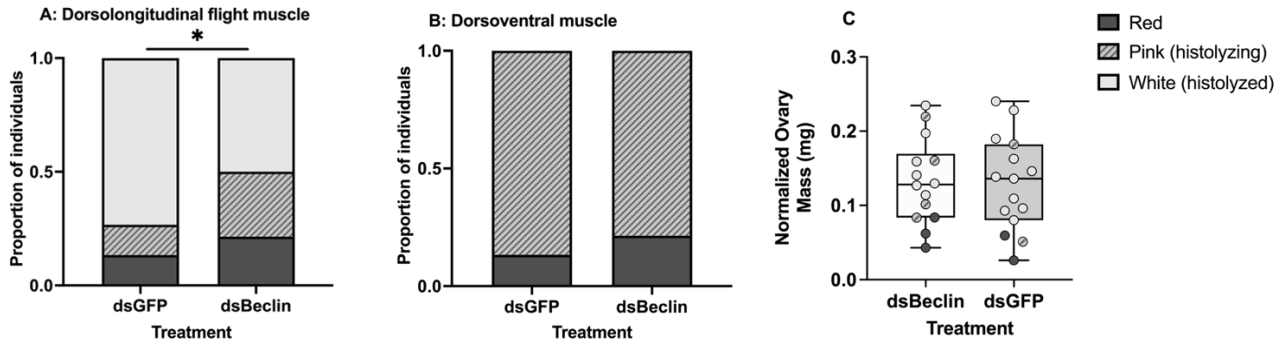

Figure 4. Knocking down *Beclin* transcript abundance delays muscle histolysis in the DLM but does not delay oogenesis in adult female *Gryllus lineaticeps*. Stacked bar graphs show the differences in the proportion of red, pink (histolyzing), and white (histolyzed) muscles in the A) dorsal longitudinal (DLM) and B) dorsoventral (DVM) flight muscles of crickets injected with either *dsBeclin* or *dsGFP*. An asterisk indicates a significant difference in frequencies between groups, according to a Fisher's exact test ($P<0.05$). C) Normalized ovary mass is similar between crickets injected with *dsBeclin* or *dsGFP*. Boxplots denote the median with whiskers denoting the minimum and maximum of ovary mass values. The solid points show individual normalized ovary masses corrected for body mass of the individual. Points are colored based on muscle color and the associated muscle status (Red: functional muscle; pink: histolyzing muscle; white: histolyzed muscle).

Because we did not observe any significant effects of knockdown on muscle histolysis in the DVM, we only measured COX and GABARAPL1/2 protein abundance in DLM. There were significantly higher levels of COX protein in the DLM of *dsBeclin* treated crickets compared to *dsGFP* treated crickets ($P = 0.0004$, $t_{14}=4.16$; Fig 5A), suggesting that knocking down *beclin* transcript abundance in female crickets prevented mitochondrial breakdown. *Beclin* knockdown also altered GABARAP protein levels, but with opposing effects on each of the Atg8-family members, GABARAPL1/2. GABARAPL1 relative protein abundance was increased ($P = 0.02$, $t_{14}=2.12$, Fig 5B), while GABARAPL2 relative protein abundance was decreased ($P = 0.02$, $t_{14}=2.22$, Fig 5C) in the DLM of crickets treated with *dsBeclin* compared to *dsGFP*.

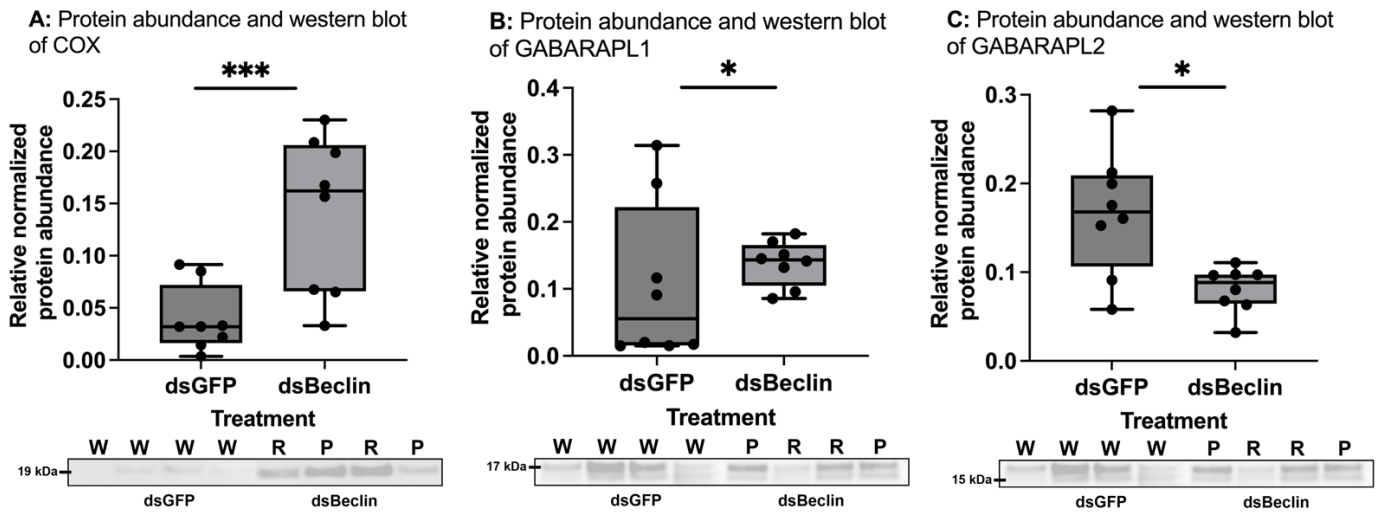

374

375 **Figure 5.** Protein abundance of cytochrome c oxidase IV (COX) and GABARAP1/2 in the
376 dorsal longitudinal (DLM) flight muscles of adult female *Gryllus lineaticeps* crickets injected
377 with *dsGFP* and *dsBeclin*. Relative normalized protein abundance of (A) COX, (B)
378 GABARAPL1, and (C) GABARAPL2 in protein lysates from DLM of *dsGFP* (n=8) and
379 *dsBeclin* (n=8) treated crickets with a representative western blot shown. Boxplots show the
380 median with whiskers showing the minimum and maximum of normalized protein abundance
381 values. Letter above sample represents color of DLM (R: Red, P: Pink, W: White). Asterisks
382 represent significant differences between treatments according to a Student's t-test (*: $P < 0.05$,
383 ***: $P < 0.001$).

384

385 **DISCUSSION**

386 Insect flight muscle histolysis is a conserved process that plays an important role in
387 modulating energetic trade-offs during important life history transitions (Zera et al. 1997; Roff
388 and Fairbairn 2007; Stahlschmidt 2022). Despite the ubiquitous nature of histolysis in at least
389 five insect orders, the molecular mechanisms driving this muscle breakdown are not well
390 understood. In this study, we examined the role of autophagy in flight muscle histolysis in adult
391 female long-winged *G. lineaticeps*. Consistent with our hypothesis, we confirmed that autophagy
392 was activated in histolyzing muscle based on the presence of autophagic structures. Although
393 these structures were present in both the dorsal longitudinal (DLM) and dorsoventral (DVM)

flight muscle, the expression of a critical autophagy-related gene, *beclin*, increases in expression in only the DLM during histolysis, suggesting autophagy is selectively activated in the DLM. To further determine the importance of autophagy in histolysis, we took an RNAi approach to experimentally knock down *beclin* transcript abundance. On the fifth day of adulthood, compared to our negative control group (*dsGFP*), the DLM of crickets injected with *dsBeclin* were less frequently histolyzed, had elevated abundance of the mitochondrial protein COX, and lower abundance of GABARAPL2, a protein activated downstream of *beclin* during autophagy. Taken together, these findings suggest that reducing *beclin* expression disrupted autophagy and promoted dorsal longitudinal flight muscle maintenance in females, providing strong support for our conclusion that autophagy acts as a key molecular mechanism driving flight muscle breakdown of insects.

Knocking down *beclin* delayed flight muscle histolysis in the DLM, but we did not observe any impacts of *beclin* knockdown on DVM histolysis. Given that *beclin* only significantly increases in expression in DLM, these results suggest that *beclin*-mediated autophagy is primarily important for DLM break-down in the time frame in which we assessed autophagy (up to five days post adult emergence). During dissections of crickets early in histolysis progression, we observed visual differences in the status and color of the DLM and DVM (see Fig 1C for example), and in our knockdown experiments, we observed complete histolysis in the DLM but not in the DVM irrespective of dsRNA treatment (Fig. 4). We therefore suggest that autophagy is differentially activated in the different groups of muscles, with DLM histolyzing first, in the first five days post adult emergence. Dorsal longitudinal muscle is primarily used for flight and DVM is used for flight and walking (Wilson 1962). It could be beneficial for crickets to decouple the timing of autophagy in both muscles such that

DVM is histolyzed later and/or to a less extent compared to DLM, especially since crickets must maintain locomotory capacity on the ground to escape predators and, when reproductively active, locate mates and find substrates for egg-laying (Dupuy et al. 2011; Samietz and Köhler 2012). We speculate that female crickets delay the onset of autophagy in DVM to maintain the clear fitness benefits of walking. Because locomotor performance declines with age in crickets, the eventual histolysis of DVM would reduce locomotor function, but at a time in their life cycle past reproduction (Faßold et al. 2010).

Because flight muscle histolysis in *G. lineaticeps* coordinates the cessation of flight with onset of large-scale oogenesis (Treidel et al. 2021; Stahlschmidt 2022), we were interested in exploring whether preventing flight muscle autophagy with RNAi also negatively impacts oogenesis. The degradation of flight muscles by autophagy may produce a pool of free amino acids that can be recycled and used for oogenesis to offset costs of the flight-for-reproduction trade-off in insects (Stjernholm et al. 2005; Treidel et al. 2023). Our results suggest autophagy may not be necessary for oogenesis because preventing *beclin*-mediated autophagy activation via RNAi knockdown did not affect ovary mass. However, since we measured ovary mass on a single day (five days post adult emergence) our data represent just a snapshot of oogenesis, and it warrants further exploration to determine if any potential effects of a *beclin* knockdown could emerge at a later point in reproductive development.

Knocking down *beclin* allowed crickets to maintain mitochondria in the DLM (as observed by maintained levels of COX protein abundance in knockdown crickets compared to non-knockdown controls), and reduced GABARAPL2 protein abundance in their DLM. Taken together, this provides evidence that crickets 1) do indeed activate autophagy during histolysis, as GABARAPL2 is involved in the later stages of activated autophagy, where it drives the

closure of the autophagosomal membrane and lysosomal fusion (Chan and Gorski 2022), and 2) that *beclin*-mediated autophagy leads to widespread mitochondrial degradation in histolyzing DLM. Mitochondria comprise a large proportion of insect flight muscle (c. 40% of cell volume; Iwamoto 2011), and mitochondria are expensive to maintain. For example, proton leak across the inner mitochondrial membrane leads to constant active ion pumping to maintain membrane potential. The dynamic nature of mitochondrial pools means that new mitochondrial proteins must be consistently synthesized (Lebenzon et al. 2023; Sokolova 2023). Thus, we propose that female *G. lineaticeps* start histolysis by selectively degrading flight muscle mitochondria (through mitochondrial-specific autophagy) to lower mitochondrial maintenance costs in their life history transition away from dispersal towards reproduction. Indeed, mitophagy is implicated in flight muscle histolysis of diapausing Colorado potato beetles (Lebenzon et al. 2022), and *beclin* has been found to play an important role in mitophagy by ensuring the proper engulfment of mitochondria by initiating autophagosome formation adjacent to the mitochondria (Quiles et al. 2023). It would be worth exploring the extent to which mitophagy contributes to muscle histolysis, in tandem with general autophagy.

Many insects activate autophagy in response to energetic challenges and unfavorable conditions. For example, autophagy allows for better heat-shock recovery in *Drosophila melanogaster* (Willot et al. 2023), drives the reduction of metabolism in diapausing Colorado potato beetles (Lebenzon et al. 2022), supports growth and differentiation during metamorphosis of *Bombyx mori* (Tian et al. 2013), and can save both *Spodoptera litura* and *Bombyx mori* cells from death during starvation (Wu et al. 2011). In all these cases, autophagy is activated in response to the need for more nutrients in poor environments and during energetic transitions, such as development and dormancy (diapause). Interestingly, female *G. lineaticeps* do not

463 necessarily activate autophagy in response to energetic challenges because histolysis is an
464 obligate part of their life cycle. Rather, it appears that *G. lineaticeps* activates autophagy in
465 anticipation of shifting energetic demands away from flight toward reproduction.
466 Overall, in determining that *beclin*-mediated autophagy drives muscle histolysis in *G.*
467 *lineaticeps* DLM, we confirmed a role of autophagy as a critical pathway used by Gryllus
468 crickets to remodel their flight muscle cells during a major life history transition between flight
469 and reproduction. Excitingly, since these crickets can selectively degrade one specific muscle
470 tissue and appear to differentially activate autophagy in muscle tissue types, future work in a
471 comparative context is warranted to elucidate how the pathological consequences of muscle
472 breakdown may mitigate or ameliorate diseases driven by aberrant rates of autophagy in humans.
473
474
475

AUTHOR CONTRIBUTIONS

TD, LAT, MAM, CMW, and JEL designed the research; TD and JEL performed the research; TD and JEL analyzed the data; TD and JEL wrote the paper, LAT, MAM and CMW contributed to the writing of the manuscript; CMW secured the funding.

ACKNOWLEDGEMENTS

The authors would like to acknowledge Savannah Wang, Andrea Neri, and Lily Donzeiser for cricket care, Robert Leilja and Jose Arevalo for assistance with western blots, Dr. Jose Vazquez-Medina for generous use of his molecular equipment, Dr. Jantina Toxopeus for dsGFP primer sequences, Reena Zalpuri and Dr. Danielle Jørgens from the Berkeley Electron Microscopy lab for assistance with transmission electron microscopy, and Dr. Meghan Laturney and Lourenço Martins for comments on earlier versions of the manuscript.

FUNDING

This work was supported by the U.S. National Science Foundation (CMW grant # 2319792), a National Sciences and Engineering Research Council of Canada Postdoctoral fellowship to JEL, and Center for Research & Education on Aging (CREA) research grant to TD.

CONFLICT OF INTEREST

The authors declare no conflicts of interest.

DATA AVAILABILITY STATEMENT

All data are available in the supplementary materials.

REFERENCES

Cao Y, Klionsky DJ. 2007. Physiological functions of Atg6/Beclin 1: a unique autophagy-related protein. Cell Res 17:839–49.

Chan JCY, Gorski SM. 2022. Unlocking the gate to GABARAPL2. Biol Futura 73:157–69.

Cheng Y, Luo L, Sappington TW, Jiang X, Zhang L, Frolov AN. 2016. Onset of oviposition triggers abrupt reduction in migratory flight behavior and flight muscle in the female beet webworm, *Loxostege sticticalis.* PLOS ONE 11:e0166859.

Dupuy F, Casas J, Body M, Lazzari CR. 2011. Danger detection and escape behaviour in wood crickets. J Insect Physiol 57:865–71.

Faßold K, El-Damanhouri HIH, Lorenz MW. 2010. Age-dependent cyclic locomotor activity in the cricket, Gryllus bimaculatus, and the effect of adipokinetic hormone on locomotion and excitability. J Comp Physiol A 196:271–83.

Goropashnaya AV, Barnes BM, Fedorov VB. 2020. Transcriptional changes in muscle of hibernating arctic ground squirrels (Urocitellus parryii): implications for attenuation of disuse muscle atrophy. Sci Rep 10:9010.

Horn T, Boutros M. 2010. E-RNAi: a web application for the multi-species design of RNAi reagents—2010 update. Nucleic Acids Res 38:W332–39.

Irschick DJ, Garland T. 2001. Locomotor Capacity as a Model System. .

Iwamoto H. 2011. Structure, function and evolution of insect flight muscle. Biophysics 7:21–28.

Kaitala, A, Hulden, L. 1990. Significance of spring migration and flexibility in flight muscle histolysis in waterstriders (Heteroptera, Gerrida). Ecol Entomol 15:409–418.

Kim J, Kundu M, Viollet B, Guan K-L. 2011. AMPK and mTOR regulate autophagy through direct phosphorylation of Ulk1. Nat Cell Biol 13:132–41.

Larsson L, Degens H, Li M, Salviati L, Lee Y il, Thompson W, Kirkland JL, Sandri M. 2019. Sarcopenia: Aging-Related Loss of Muscle Mass and Function. Physiol Rev 99:427–511.

Lebenzon JE, Denezis PW, Mohammad L, Mathers KE, Turnbull KF, Staples JF, Sinclair BJ. 2022. Reversible mitophagy drives metabolic suppression in diapausing beetles. Proc Natl Acad Sci 119:e2201089119.

Lebenzon JE, Overgaard J, Jørgensen LB. 2023. Chilled, starved or frozen: insect mitochondrial adaptations to overcome the cold. Curr Opin Insect Sci 58: 101076.

Livak KJ, Schmittgen TD. 2001. Analysis of Relative Gene Expression Data Using Real-Time Quantitative PCR and the 2−ΔΔCT Method. Methods 25:402–8.

Lorenz MW. 2007. Oogenesis-flight syndrome in crickets: Age-dependent egg production, flight performance, and biochemical composition of the flight muscles in adult female *Gryllus bimaculatus*. J Insect Physiol, VIII European Congress of Entomology - Physiology and Endocrinology 53:819–32.

Lu Y, Wang Z, Lin F, Ma Y, Kang J, Fu Y, Huang M, Zhao Z, Zhang J, Chen Q, Ren B. 2023. Screening and identification of genes associated with flight muscle histolysis of the house cricket Acheta domesticus. Front Physiol 13.

Matte A, Billen J. 2021 Flight muscle histolysis in Lasius niger queens. Asian Myrmecology 13: e013003.

Marden JH. 2000. Variability in the Size, Composition, and Function of Insect Flight Muscles. Annu Rev Physiol 62:157–78.

Mizushima N. 2007. Autophagy: process and function. Genes Dev 21:2861–73.

Nespolo RF, Roff DA, Fairbairn DJ. 2008. Energetic trade-off between maintenance costs and flight capacity in the sand cricket (Gryllus firmus). Funct Ecol 22:624–31.
Pinet K, McLaughlin KA. 2019. Mechanisms of physiological tissue remodeling in animals: Manipulating tissue, organ, and organism morphology. Dev Biol 451:134–45.
Price ER, Bauchinger U, Zajac DM, Cerasale DJ, McFarlan JT, Gerson AR, McWilliams SR, Guglielmo CG. 2011. Migration- and exercise-induced changes to flight muscle size in migratory birds and association with IGF1 and myostatin mRNA expression. J Exp Biol 214:2823–31.
Quiles JM, Najor RH, Gonzalez E, Jeung M, Liang W, Burbach SM, Zumaya EA, Diao RY, Lampert MA, Gustafsson ÅB. 2023. Deciphering functional roles and interplay between Beclin1 and Beclin2 in autophagosome formation and mitophagy. Sci Signal 16:eabo4457.
Roff DA, Fairbairn DJ. 2007. The evolution of trade-offs: where are we? J Evol Biol 20:433–47.
Romanello V, Sandri M. 2016. MITOCHONDRIA QUALITY CONTROL AND MUSCLE MASS MAINTENANCE. Front Physiol 6.
Samietz J, Köhler G. 2012. A fecundity cost of (walking) mobility in an insect. Ecol Evol 2:2788–93.
Schaaf MBE, Keulers TG, Vooijs MA, Rouschop KMA. 2016. LC3/GABARAP family proteins: autophagy-(un)related functions. FASEB J 30:3961–78.
Shiga S, Yasuyama K, Okamura N, Yamaguchi T. 2002. Neural- and endocrine control of flight muscle degeneration in the adult cricket, *Gryllus bimaculatus*. J Insect Physiol 48:15–24.
Sokolova IM. 2023. Ectotherm mitochondrial economy and responses to global warming. Acta Physiol 237:e13950.
Stahlschmidt ZR. 2022. Flight capacity drives circadian patterns of metabolic rate and alters resource dynamics. J Exp Zool Part Ecol Integr Physiol 337:666–74.
STJERNHOLM F, KARLSSON B, BOGGS CL. 2005. Age-related changes in thoracic mass: possible reallocation of resources to reproduction in butterflies. Biol J Linn Soc 86:363–80.
Sun Q, Fan W, Zhong Q. 2009. Regulation of Beclin 1 in autophagy. Autophagy 5:713–16.
Tian L, Ma L, Guo E, Deng X, Ma S, Xia Q, Cao Y, Li S. 2013. 20-hydroxyecdysone upregulates Atg genes to induce autophagy in the Bombyx fat body. Autophagy 9:1172–87.
Treidel LA, Clark RM, Lopez MT, Williams CM. 2021. Physiological demands and nutrient intake modulate a trade-off between dispersal and reproduction based on age and sex of field crickets. J Exp Biol 224:jeb237834.
Treidel LA, Goswami P, Williams CM. 2023. Changes in mitochondrial function parallel life history transitions between flight and reproduction in wing polymorphic field crickets. Am J Physiol-Regul Integr Comp Physiol 324:R735–46.
Treidel LA, Huebner C, Roberts KT, Williams CM. 2022. Life history strategy dictates thermal preferences across the diel cycle and in response to starvation in variable field crickets, *Gryllus lineaticeps*. Curr Res Insect Sci 2:100038.
Vellichirammal NN, Zera AJ, Schilder RJ, Wehrkamp C, Riethoven JM, Brisson JA. *De novo* transcriptome assembly from fat body and flight muscle transcripts to identify morph-specific gene expression profiles in *Gryllus firmus*. PLOS ONE 9:e82129.
Wall BT, Dirks ML, van Loon LJC. 2013. Skeletal muscle atrophy during short-term disuse: Implications for age-related sarcopenia. Ageing Res Rev 12:898–906.

Weis-Fogh T. 1964. Diffusion in Insect Wing Muscle, the Most Active Tissue Known. J Exp Biol 41:229–56.
Wheeler D. 1996. The Role of Nourishment in Oogenesis. Annu Rev Entomol 41:407–31.
Willot Q, du Toit A, de Wet S, Huisamen EJ, Loos B, Terblanche JS. 2023. Exploring the connection between autophagy and heat-stress tolerance in Drosophila melanogaster. Proc R Soc B Biol Sci 290:20231305.
Wilson DM. 1962. Bifunctional Muscles in the Thorax of Grasshoppers. J Exp Biol 39:669–77.
Wu W, Wei W, Ablimit M, Ma Y, Fu T, Liu K, Peng J, Li Y, Hong H. 2011. Responses of two insect cell lines to starvation: Autophagy prevents them from undergoing apoptosis and necrosis, respectively. J Insect Physiol 57:723–34.
Ylla G, Nakamura T, Itoh T, Kajitani R, Toyoda A, Tomonari S, Bando T, Ishimaru Y, Watanabe T, Fuketa M, Matsuoka Y, Barnett AA, Noji S, Mito T, Extavour CG. 2021. Insights into the genomic evolution of insects from cricket genomes. Commun Biol 4:1–12.
Young KG, Regnault TRH, Guglielmo CG. 2021. Extraordinarily rapid proliferation of cultured muscle satellite cells from migratory birds. Biol Lett 17:20210200.
Zera AJ, Potts J, Kobus K. 1998. The Physiology of Life-History Trade-offs: Experimental Analysis of a Hormonally Induced Life-History Trade-off in Gryllus assimilis. Am Nat 152:7–23.
Zera AJ, Sall J, Grudzinski K. 1997. Flight-Muscle Polymorphism in the Cricket *Gryllus firmus:* Muscle Characteristics and Their Influence on the Evolution of Flightlessness. Physiol Zool 70:519–29.
Zhang Y, Tessier SN, Storey KB. 2016. Inhibition of skeletal muscle atrophy during torpor in ground squirrels occurs through downregulation of MyoG and inactivation of Foxo4. Cryobiology 73:112–19.